J Appl Electrochem (2008) 38:1127–1133
DOI 10.1007/s10800-008-9574-7

ORIGINAL PAPER

Electrochemical promotion of CO_2 hydrogenation on Rh/YSZ electrodes

S. Bebelis · H. Karasali · C. G. Vayenas

Received: 19 December 2007 / Revised: 17 April 2008 / Accepted: 18 April 2008 / Published online: 6 May 2008

Abstract The electrochemical promotion of the CO_2 hydrogenation reaction on porous Rh catalyst–electrodes deposited on Y_2O_3-stabilized-ZrO_2 (or YSZ), an O^{2-} conductor, was investigated under atmospheric total pressure and at temperatures 346–477 °C, combined with kinetic measurements in the temperature range 328–391 °C. Under these conditions CO_2 was transformed to CH_4 and CO. The CH_4 formation rate increased by up to 2.7 times with increasing Rh catalyst potential (electrophobic behavior) while the CO formation rate was increased by up to 1.7 times with decreasing catalyst potential (electrophilic behavior). The observed rate changes were non-faradaic, exceeding the corresponding pumping rate of oxygen ions by up to approximately 210 and 125 times for the CH_4 and CO formation reactions, respectively. The observed electrochemical promotion behavior is attributed to the induced, with increasing catalyst potential, preferential formation on the Rh surface of electron donor hydrogenated carbonylic species leading to formation of CH_4 and to the decreasing coverage of more electron acceptor carbonylic species resulting in CO formation.

Keywords Electrochemical promotion · NEMCA Effect · CO_2 Hydrogenation · Rhodium · Rh · YSZ

S. Bebelis (✉) · H. Karasali · C. G. Vayenas
Department of Chemical Engineering, University of Patras, 26504 Patras, Greece
e-mail: simeon@chemeng.upatras.gr

Present Address:
H. Karasali
Benaki Phytopathological Institute, 8 St. Delta Str., 14561 Athens, Greece

1 Introduction

The catalytic properties of metal and metal-oxide porous catalyst–electrode films deposited on ionic conductors can be reversibly altered in a very pronounced and controlled manner by electrically polarizing of the catalyst–electrode via the effect of electrochemical promotion of catalysis (EPOC) or non-faradaic electrochemical modification of catalytic activity (NEMCA effect) [1–4]. A key finding in the interpretation of the EPOC effect is the variation of the catalyst–electrode work function upon polarization, with concomitant changes in the binding strength of chemisorbed species and reaction intermediates [3, 4]. These changes result in rate changes exceeding the corresponding rate of ion transport through the ionic conductor (non-faradaic changes), even by several orders of magnitude [1–4]. Work in this area has recently been reviewed [4].

EPOC has been studied in a number of hydrogenation reactions [4], including CO_2 hydrogenation reaction under atmospheric pressure over Cu interfaced to $SrZr_{0.9}Y_{0.1}O_{3-\alpha}$, a proton conductor [5], over Pt interfaced to ZrO_2 (8 mol%Y_2O_3) or YSZ, an O^{2-} conductor [6] and over Pd interfaced to YSZ or β''-Al_2O_3, a sodium ion conductor [4, 7]. The present work concerns the electrochemical promotion of the CO_2 hydrogenation reaction over Rh catalyst–electrodes interfaced to YSZ, combined with kinetic measurements, under atmospheric pressure and at temperatures 328–477 °C. Under these conditions the carbon-containing reaction products were CO and CH_4. A short reference on this study has first appeared in a recent review [4].

2 Experimental

The experiments were carried out in a continuous flow apparatus which has been described previously [4, 8]. The

flow of gases was controlled by a set of calibrated flowmeters (Brooks 5878). Pure H_2 and CO_2, with N_2 as balance gas, were used in the kinetic experiments while certified standards of H_2 in He and CO_2 in He (Messer-Griesheim), with He as balance gas, were used in the EPOC experiments. CO, CO_2, CH_4 and H_2 (for partial pressures lower approximately than 2 kPa) were analyzed by on-line gas chromatography (Shimadzu 14B gas chromatograph with TCD and FID), using a Porapak QS (at 35 °C) and a Carbosieve-S-II (at 110 °C) packed columns. The presence of H_2O in the products was identified (Porapak QS column at 140 °C) but not quantified in all cases. A fuel cell type reactor [4, 8] with a three electrode set-up was used, where the reaction was carried out in the inner side of an YSZ tube (Zircoa, Inc, 19.5 mm O.D., 15.5 mm I.D., 15 cm length).

The Rh catalyst–electrodes were porous with thicknesses on the order of a few μm. They were deposited on the inner bottom side of the YSZ tube by application of thin coatings of Engelhard 6894 Rh paste, followed by calcination in air, first at 400 °C (5 °C min^{-1}) for 2 h and then at 950 °C (5 °C min^{-1}) for 30 min. The electrodes were finally reduced at 240 °C for 16 h under flow of 2% H_2 in He mixture. The porous Pt counter and reference electrodes were exposed to ambient air. They were deposited on the outer bottom side of the YSZ tube, opposite to the Rh catalyst–electrode, by application of thin coatings of Engelhard A1121 Pt paste followed by calcination in air, first at 400 °C (5 °C min^{-1}) for 2 h and then at 830 °C (7 °C min^{-1}) for 20 min. The surface mol (mol of active sites) N of the Rh electrodes (geometric area $\approx$ 1.8 cm^2) were determined via comparison of their catalytic activity under certain conditions with that of a Rh electrode the surface mol of which were determined via hydrogen chemisorption at 60 °C, in the hydrogen pressure range 1–15 Torr, assuming an 1:1 hydrogen to rhodium adsorption stoichiometry.

Constant potentials between the Rh catalyst and the Pt reference electrode or constant currents between the Rh catalyst and the Pt counter electrode were applied via an AMEL 553 galvanostat–potentiostat. The ohmic drop free catalyst potential U_{WR} was obtained by subtracting the ohmic drop component, determined via the current interruption technique [4], from the measured catalyst potential value U'_{WR}.

3 Results

Figure 1a–d shows, for catalyst–electrode R3 ($N = 4.2 \times 10^{-6}$ mol Rh), the effect of H_2 and CO_2 partial pressures on the regular, i.e., open-circuit, catalytic rate of CH_4 (Fig. 1a, b) and CO (Fig. 1c, d) formation. The total flow rate was between 15 and 50 cm^3 (STP) min^{-1}. The rate of CH_4 formation increases initially with increasing hydrogen or CO_2 partial pressure reaching a plateau beyond a certain partial pressure value, which depends on temperature. On the other hand, the rate of CO formation increases linearly with increasing H_2 or CO_2 partial pressure. This behavior is in agreement with a mechanism which includes formation

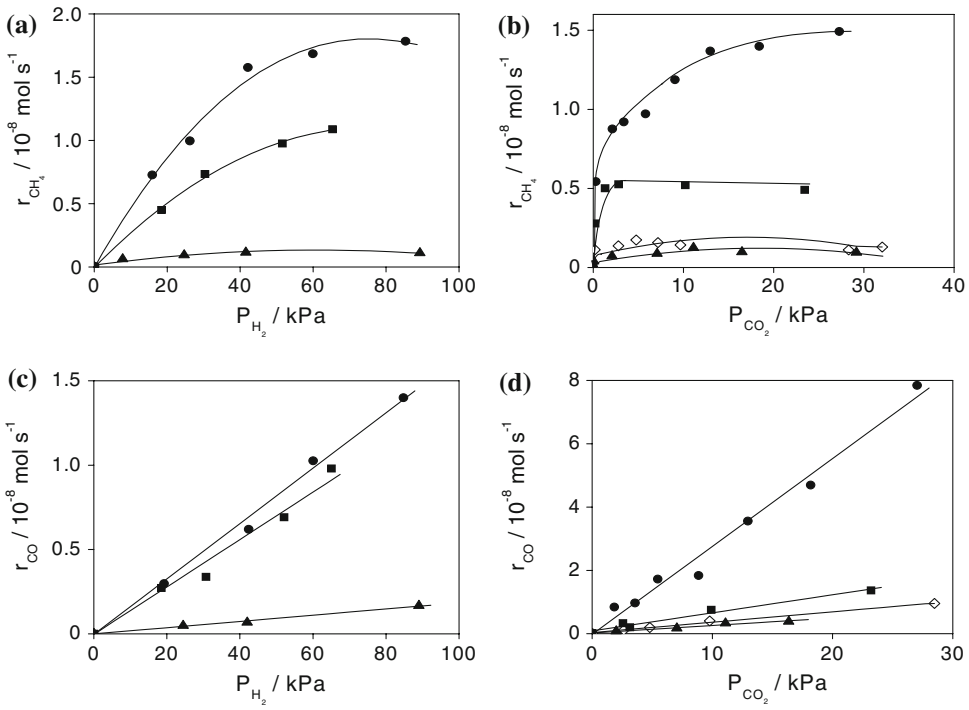

Fig. 1 Dependence of the CH_4 (**a**, **b**) and CO (**c**, **d**) formation rates on P_{H_2} at P_{CO_2} = 5.5 kPa and on P_{CO_2} at P_{H_2} = 63 kPa. Catalyst–electrode R3 ($N = 4.2 \times 10^{-6}$ mol Rh). Flow rate 15–50 cm^3 (STP) min^{-1}. (▲) 328°C, (◇) 355 °C, (■) 372 °C, (●) 391 °C

of CO in the first step and dissociation of CO in the rate determining step for CH_4 production via interaction of the carbon species with adsorbed hydrogen [9].

Figure 2a, b shows, for catalyst–electrode R3, the effect of H_2 and CO_2 partial pressures on the open-circuit catalyst potential $U_{WR,o}$. The potential increases with increasing temperature, while it decreases (becomes more negative) with increasing hydrogen partial pressure P_{H_2} (Fig. 2a) and increases with increasing CO_2 partial pressure P_{CO_2} (Fig. 2b). This behavior implies that H_2 is adsorbed on the Rh electrode surface as an electron donor, lowering its work function and thus lowering its potential [3, 4] and, also, that CO_2 is adsorbed on the Rh electrode surface as an electron acceptor, increasing the catalyst work function and thus increasing its potential [3, 4]. The observed increase in the open-circuit potential with increasing temperature can be attributed to change in the relative coverage of the electron donor and electron acceptor species, the adsorption of the latter, including spillover oxygen ions from the YSZ [3, 4], being here favored at higher temperatures.

Figure 3a, b shows, for catalyst–electrode R4 ($N = 6 \times 10^{-6}$ mol Rh), the dependence of the rates of methane and CO formation, respectively, on hydrogen partial pressure P_{H_2}, at constant $P_{CO_2} = 10$ kPa and T = 346 °C, under open-circuit conditions and when the catalyst potential is maintained at −0.8 V (application of positive overpotentials) or at −1.6 V (application of negative overpotentials). The kinetic effect of hydrogen does not change significantly under closed-circuit (EPOC) conditions, especially concerning the methanation reaction. Furthermore, over the entire range of hydrogen partial pressures the rate of methane formation increases with increasing catalyst potential (Fig. 3a), i.e. electrophobic EPOC behavior [4] is observed, while the rate of CO formation increases with

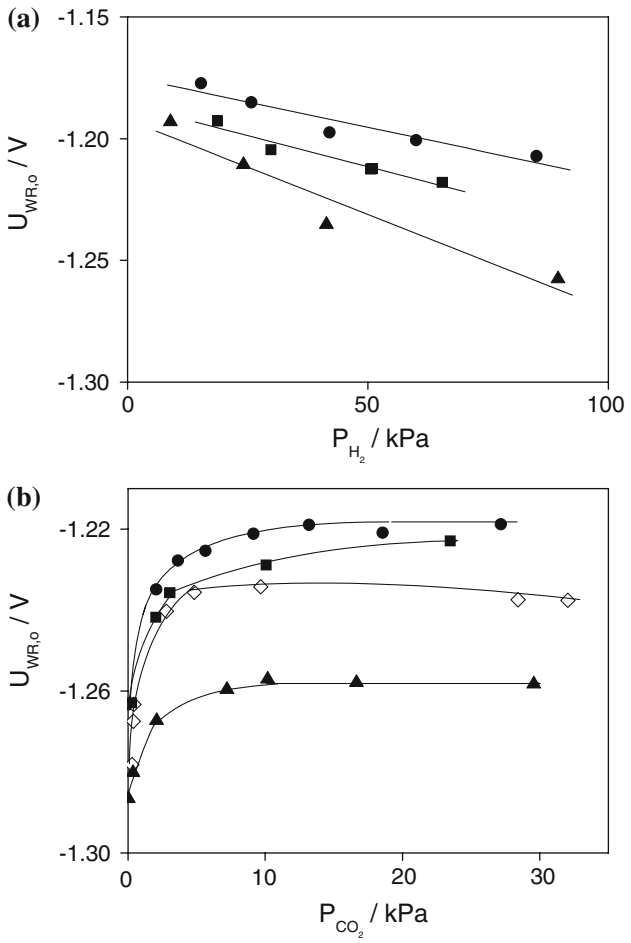

Fig. 2 Dependence of the open circuit catalyst potential $U_{WR,o}$ on P_{H_2} at $P_{CO_2} = 5.5$ kPa (**a**) and on P_{CO_2} at $P_{H_2} = 63$ kPa (**b**). Catalyst–electrode R3 ($N = 4.2 \times 10^{-6}$ mol Rh). (▲) 328 °C, (◇) 355 °C, (■) 372 °C, (●) 391 °C

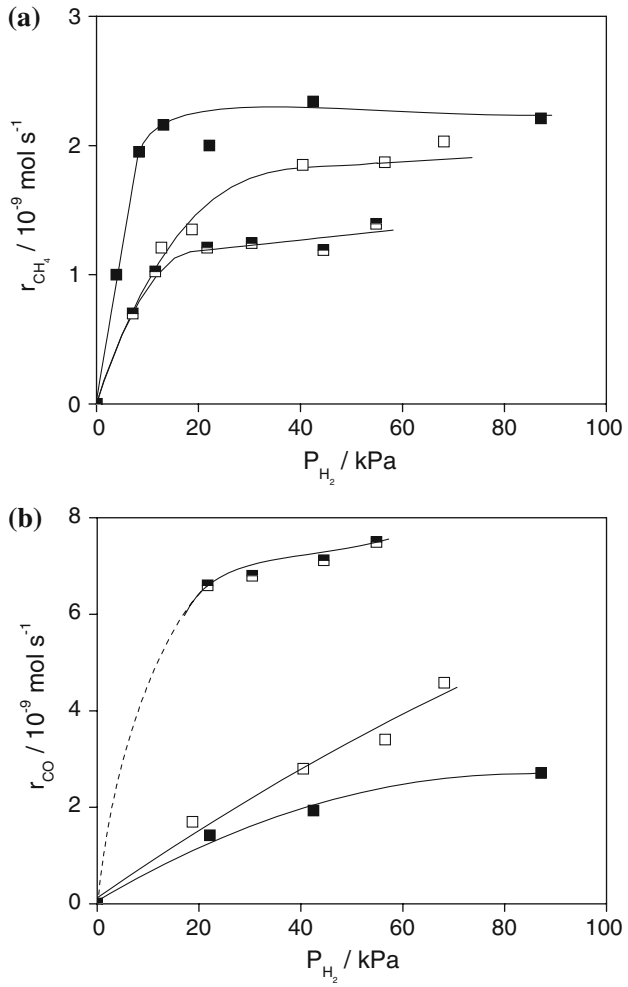

Fig. 3 Comparison of the dependence of the CH_4 (**a**) and CO (**b**) production rates on P_{H_2} at $P_{CO_2} = 10$ kPa under open-circuit (open symbols) and closed-circuit conditions, where ■: $U'_{WR} = -0.8$ V (positive overpotential) and ⬒: $U'_{WR} = -1.6$ V (negative overpotential). T = 346 °C. Catalyst–electrode R4 ($N = 6 \times 10^{-6}$ mol Rh). Flow rate 43–50 cm^3 (STP) min^{-1}

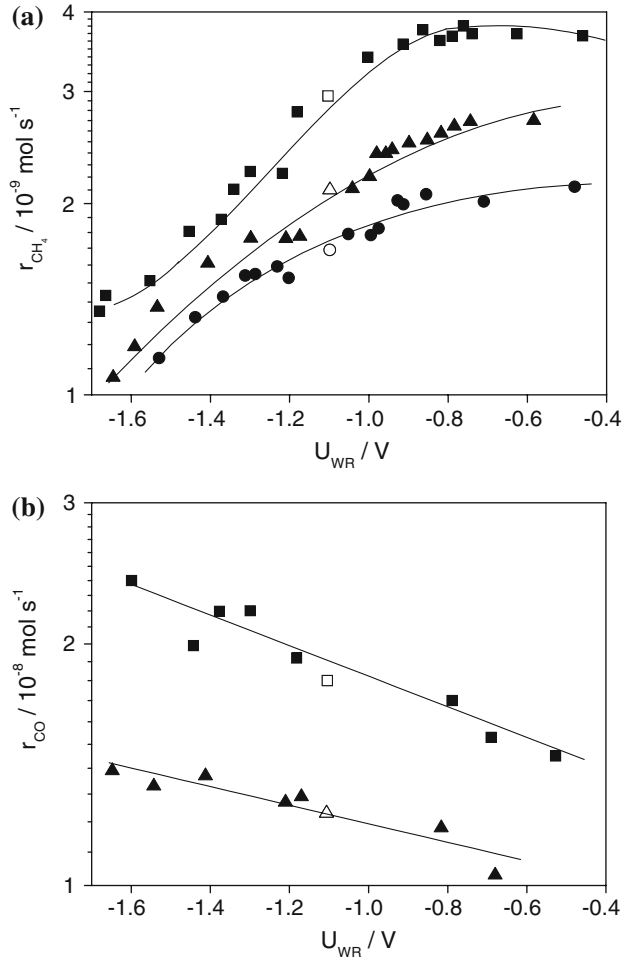

Fig. 4 Effect of catalyst potential U_{WR} on the CH_4 production rate (**a**) and on the CO production rate (**b**) for catalyst–electrode R1 ($N = 3.9 \times 10^{-7}$ mol Rh). Open symbols correspond to open-circuit conditions. $P_{CO_2} = 1$ kPa, $P_{H_2} = 1.5$ kPa. (●) 400 °C (flow rate 27 cm^3 (STP) min^{-1}), (▲) 451 °C (flow rate 38 cm^3 (STP) min^{-1}), (■) 468 °C (flow rate 38.5 cm^3 (STP) min^{-1})

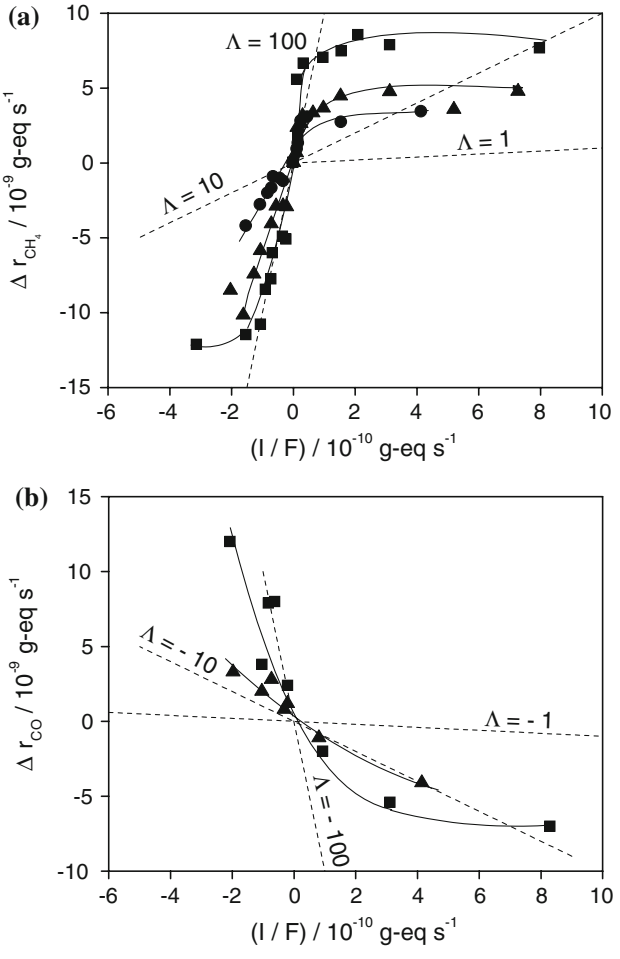

Fig. 5 Effect of the oxygen ion transfer rate I/F on the CH_4 (**a**) and CO (**b**) production rate changes. Catalyst–electrode R1 ($N = 3.9 \times 10^{-7}$ mol Rh). Conditions as in Fig. 4. Dashed lines are constant enhancement factor Λ lines

decreasing catalyst potential (Fig. 3b), i.e. electrophilic EPOC behavior [4] is observed.

Figure 4a, b shows the effect of the ohmic-drop-free catalyst potential U_{WR} on the rate of CH_4 and CO production for catalyst–electrode R1 ($N = 3.9 \times 10^{-7}$ mol Rh) in the temperature range 400–468 °C and for a P_{H_2}/P_{CO_2} ratio equal to 1.5. The experiments were carried out galvanostatically. As shown in the figures, with increasing catalyst potential by approximately 1.1 V (T = 468 °C) the CH_4 formation rate increases (electrophobic EPOC behavior [4]) by up to 2.7 times and the CO formation rate decreases (electrophilic EPOC behavior [4]) by up to 1.7 times. The induced rate changes are non faradaic. This is shown in Fig. 5a, b where is depicted the effect of O^{2-} pumping rate I/F, expressed in g-eq s^{-1}, on the induced CH_4 (Fig. 5a) and CO (Fig. 5b) formation rate changes, also expressed in g-eq s^{-1}, i.e. $\Delta r_{CH_4}(\text{g-eq s}^{-1}) = 8\,\Delta r_{CH_4}(\text{mol s}^{-1})$ and $\Delta r_{CO}(\text{g-eq s}^{-1}) = 2\,\Delta r_{CO}(\text{mol s}^{-1})$. Absolute values of the faradaic efficiency or enhancement factor $\Lambda_i = \Delta r_i\,(\text{g-eq s}^{-1})/(\text{I/F})$ [3, 4, 8] up to approximately 210 and 125 were measured for the CH_4 and CO formation reactions, respectively.

Qualitatively the same behavior was observed using a second catalyst film (catalyst–electrode R2) with surface mol $N = 3.1 \times 10^{-7}$ mol Rh, in the temperature range 425–477 °C and for a P_{H_2}/P_{CO_2} ratio equal to 1.8. The corresponding results are presented in Figs. 6 and 7. In this case only experiments corresponding to negative current application were carried out. As shown in Fig. 6a, b, the rate of methane production is reduced by up to a factor of 0.4 with decreasing catalyst potential by approximately 0.5 V (T = 477 °C). At the same time the CO formation rate increases by up to approximately 27%. The induced rate changes are non faradaic (Figs. 7a, b) with corresponding absolute values of the enhancement

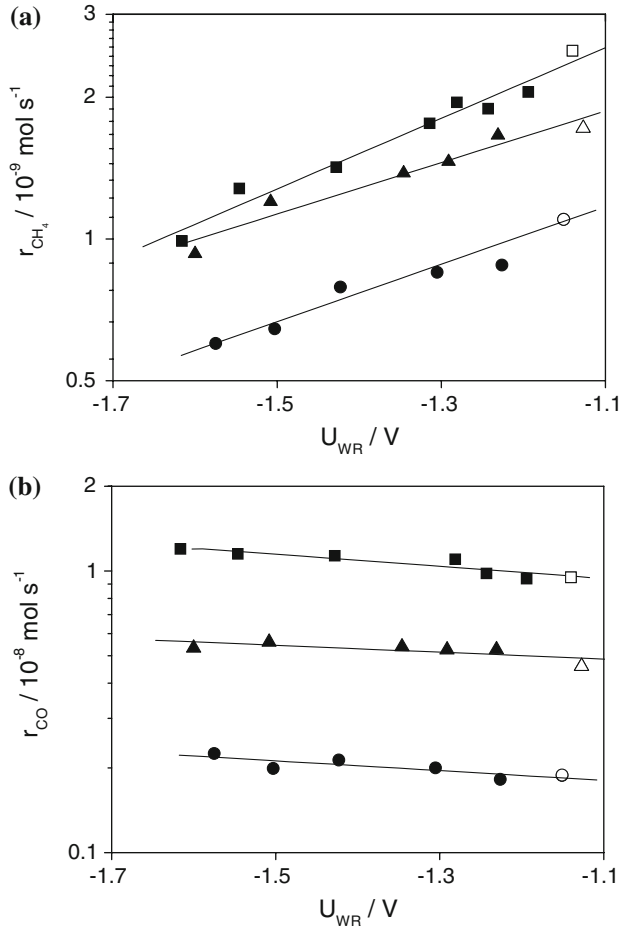

Fig. 6 Effect of catalyst potential U_{WR} on the CH_4 production rate (**a**) and on the CO production rate (**b**) for catalyst–electrode R2 ($N = 3.1 \times 10^{-7}$ mol Rh). Open symbols correspond to open-circuit conditions. $P_{CO_2} = 1$ kPa, $P_{H_2} = 1.8$ kPa. (●) 425 °C (flow rate 37 cm^3 (STP) min^{-1}), (▲) 447 °C (flow rate 34 cm^3 (STP) min^{-1}), (■) 477 °C (flow rate 37.8 cm^3 (STP) min^{-1})

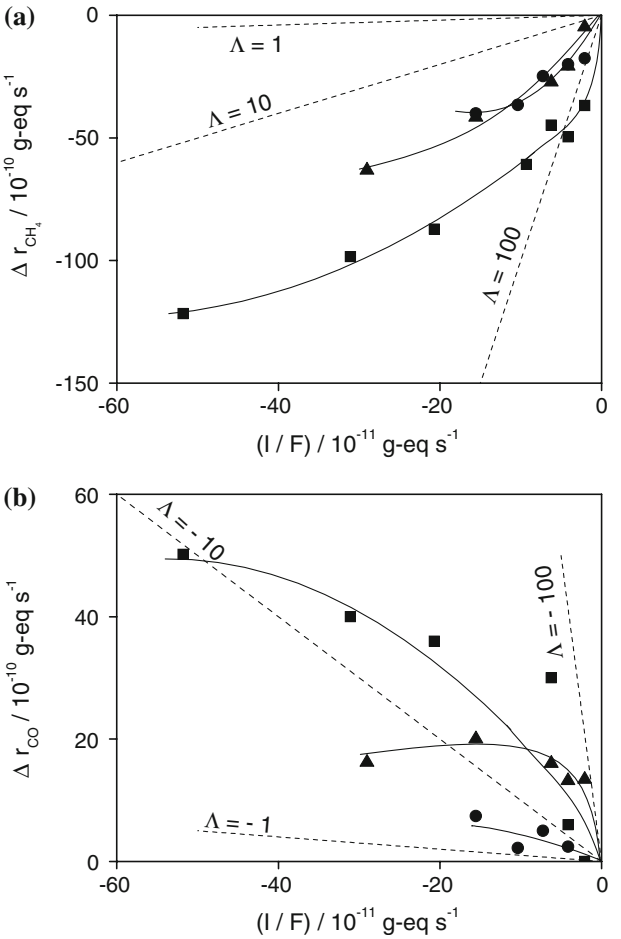

Fig. 7 Effect of the oxygen ion transfer rate I/F on the CH_4 (**a**) and CO (**b**) production rate changes. Catalyst–electrode R2 ($N = 3.1 \times 10^{-7}$ mol Rh). Conditions as in Fig. 6. Dashed lines are constant enhancement factor Λ lines

factor Λ_i up to 178 and 65 for the CH_4 and CO formation reactions, respectively.

Figure 8a, b shows the effect of catalyst potential U_{WR} on the selectivity of CH_4 formation for catalyst–electrodes R1 (Fig. 8a) and R2 (Fig. 8b) for which the open-circuit selectivity values varied from 14.1% to 14.6% and from 21% to 37%, respectively, depending on temperature (selectivity to methane decreases with increasing temperature). As expected from the effect of U_{WR} on the CH_4 and CO production rates (Figs. 4 and 6), the selectivity to methane increases with positive current application, by up to approximately 38% (catalyst R1, T = 468 °C) for an increase in the catalyst potential by 0.45 V (Fig. 8a), while it decreases with negative current application, by up to a factor of 0.37 (catalyst R2, T = 477 °C) for a decrease in catalyst potential by 0.48 V (Fig. 8b).

4 Discussion

The observed electrochemical promotion behavior can be rationalized by taking into account the effect of changing catalyst potential on catalyst work function Φ [3, 4] and, thus, on the strength of the chemisorptive bond of the reactive surface species (reactants and reaction intermediates), in view of the prevailing ideas concerning the mechanism of the CO_2 hydrogenation reaction on Rh [9].

Both H_2 and CO_2 are adsorbed dissociatively on the Rh surface [10–12], the dissociation of CO_2 being considerably enhanced by the presence of hydrogen [10–12], as also implied by the observed increase in the CO production rate with increasing hydrogen partial pressure (Fig. 1c). CO resulting from the adsorption of CO_2 can be desorbed in the gas phase or dissociated further into adsorbed oxygen and reactive (carbidic) surface carbon species [9]. Gradual hydrogenation of the latter species results finally in methane formation, while H_2O is also formed by

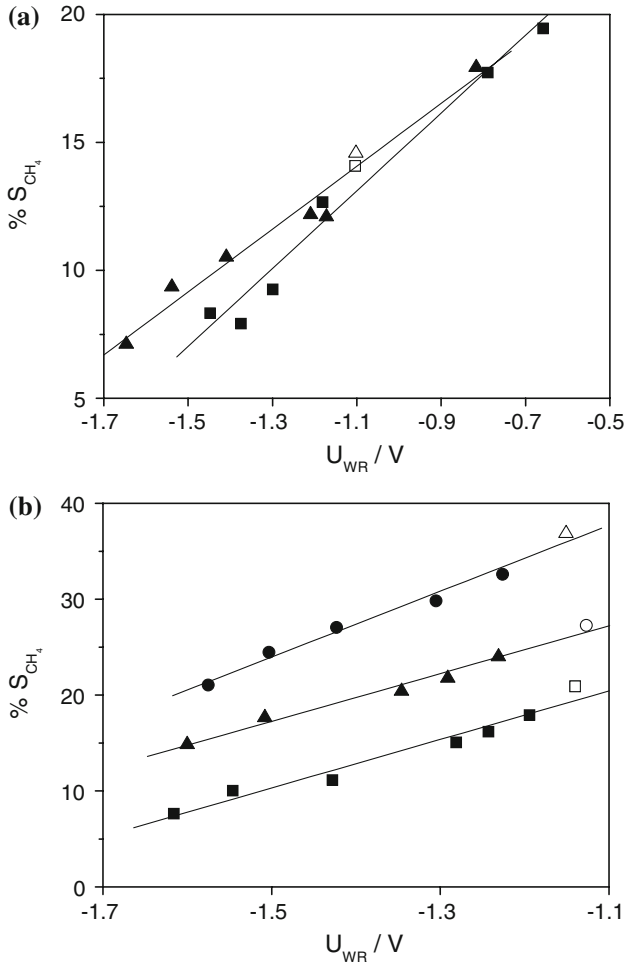

Fig. 8 Effect of catalyst potential U_{WR} on the selectivity of CH_4 production. (**a**) Catalyst–electrode R1, (▲) 451 °C, (■) 468 °C. Conditions as in Fig. 4. (**b**) Catalyst–electrode R2, (●) 425 °C, (▲) 447 °C, (■) 477 °C. Conditions as in Fig. 6

reaction between the adsorbed hydrogen and oxygen species [9]. Infrared spectroscopic studies of the adsorption and reaction of CO_2 and H_2 over supported Rh [10–12] have shown that CO_2 adsorption in the presence of H_2 results in formation of both rhodium carbonyl species, which are the intermediates for CO formation and rhodium carbonyl mono- or di-hydride species, which are the intermediates for CH_4 formation. In the latter species the electron donation from hydrogen into the π^* orbitals of the CO moiety results in loosening of the C–O intermolecular bond and enhancement of the CO dissociation, which is considered [9] the key step for CH_4 formation. As hydrogen exhibits electron donor behavior (Fig. 2a), increase of the catalyst potential and work function [3, 4] enhances its interaction with the Rh surface and thus favors the formation of the rhodium carbonyl hydride species compared to that of the rhodium carbonyl species. As a result the methanation rate increases and the CO production rate decreases. The opposite behavior is observed when decreasing catalyst potential and can be explained on the basis of the same arguments.

On the basis of the results of the kinetic experiments depicted in Figs. 1a, b and 3a, under the conditions of the electrochemical promotion experiments of the present study (Figs. 4–8) the kinetics of the methanation reaction are expected to be first order in H_2, the electron donor reactant, and zero order in CO_2, the electron acceptor reactant. Thus, the observed electrophobic behavior for this reaction is in agreement with the rules derived by Vayenas et al. [13] for predicting the chemical and electrochemical promotion behavior on the basis of open circuit kinetics taking into account the electron acceptor or electron donor nature of the reactants.

5 Conclusions

The present study shows that EPOC can affect the reaction of CO_2 hydrogenation on Rh films interfaced to YSZ, both concerning catalytic rates and selectivity to the reactions products. In the temperature range 346–477 °C and under atmospheric total pressure, where the carbon-containing products were CH_4 and CO, with increasing catalyst potential by approximately 1.1 V the methanation rate was enhanced (electrophobic EPOC behavior [4]) by up to 2.7 times while the rate of CO production decreased (electrophilic EPOC behavior [4]) by up to 1.7 times. The observed rate changes were non-faradaic exceeding the corresponding electrocatalytic rate by up to approximately 210 and 125 times for the CH_4 and CO formation reactions, respectively. The exhibited electrochemical promotion behavior can be explained by taking into account the mechanism of the reaction and the effect of catalyst potential on the relative propensity of formation of the different intermediate species which lead to formation of CH_4 or CO, depending on their electron donor or electron acceptor nature.

References

1. Lintz HG, Vayenas CG (1989) Angew Chem Int Ed Engl 28(6):708
2. Vayenas CG, Bebelis S, Neophytides S, Yentekakis IV (1989) Appl Phys A 49:95
3. Vayenas CG, Bebelis S, Ladas S (1990) Nature 343:625
4. Vayenas CG, Bebelis S, Pliangos C, Brosda S, Tsiplakides D, (2001) In: Electrochemical activation of catalysis: promotion, electrochemical promotion and metal-support interactions. Kluwer Academic Publishers/Plenum Press, New York
5. Karagiannakis G, Zisekas S, Stoukides M (2003) Solid State Ionics 162–163:313
6. Pekridis G, Kalimeri K, Kaklidis N, Vakouftsi E, Iliopoulou EF, Athanasiou C, Marnellos GE (2007) Catal Tod 27:337

7. Bebelis S, Karasali H, Vayenas CG (2008) Solid State Ionics. doi: 10.1016/j.ssi.2008.02.043
8. Bebelis S, Vayenas CG (1989) J Catal 118:125
9. Solymosi F, Erdohelyi A, Bansagi T (1981) J Catal 68:371
10. Solymosi F, Knözinger H (1990) J Catal 122:166
11. Henderson MA, Worley SD (1985) Surf Sci 149:L1
12. Solymosi F, Pasztor M (1987) J Catal 104:312
13. Vayenas CG, Brosda S, Pliangos C (2001) J Catal 203:329